DOI 10.5162/Ultrasonic2025/E2-a2

Neural network method for inversion of S-wave velocity in soft formation from monopole acoustic logging signals

Wanting Lin[1] *and Hengshan Hu*[1]
[1]*Harbin Institute of Technology, Harbin, Heilongjiang, China*
hhs@hit.edu.cn

Abstract: It is generally believed that the monopole acoustic logging cannot be used to invert the S-wave velocity in a soft formation. However, the theoretically synthesized pressure waveform of monopole acoustic logging changes obviously with S-wave velocity, indicating a correlation between the two. This paper uses one-dimensional convolution neural network to invert the S-wave velocity. In the absence of dipole S-wave logging data, S-wave velocity is inverted with less than 2% error through the full waveform of monopole acoustic logging.

Keywords: neural network, S-wave velocity, soft formation, monopole acoustic logging, borehole.

Introduction

S-wave velocity serves as an important basis for calculating rock mechanics parameters, stress parameters, and formation anisotropy. It is still necessary to predict S-wave velocity using monopole logging data [1]. Although dipole acoustic logging is currently employed, a large amount of existing old data only contains monopole logging data. Hence, accurately obtaining S-wave velocity is of crucial importance. It is generally believed that the critically refracted S-wave arrivals cannot be received in boreholes within soft formations. Although it has been proven that critically refracted S-waves can exist in boreholes within soft formations [2], such inhomogeneous waves attenuate rapidly as they move away from the borehole wall, making them difficult to be detected by receivers located on the borehole axis. Wu [3] used the low - frequency approximate formula of Stoneley wave velocity obtained under different formation medium models and logging sonde configurations to invert the formation S-wave velocity. However, when the source frequency is higher than 5 kHz or in the case of a harder formation, this approximate formula cannot effectively reflect the relationship between the Stoneley wave velocity and the S-wave velocity. Cheng [4] proposed a method for obtaining S-wave velocity from critically refracted P-waves in acoustic logging within formations where critically refracted S-waves or pseudo-Rayleigh waves do not exist. However, when there are errors in the input parameters when the input parameters of the inversion algorithm (such as P-wave velocity and formation density) are not accurate enough, the accuracy of the inverted S-wave velocity will also decrease. The works documented in references [3][4] represent efforts to invert for S-wave velocity in scenarios where independent S-waves or pseudo-Rayleigh waves are unavailable. However, relying solely on individual characteristics of the full waveform makes it challenging to achieve S-wave velocity inversion with sufficient accuracy, as the one-to-one correspondence between these individual full-waveform features and S-wave velocity remains unclear. For this reason, this paper avoids individual characteristics of the waveform and attempts to invert the S-wave velocity from the entire wave train itself.

This paper leverages a one-dimensional convolutional neural network (1D-CNN) [5] to address the issue of S-wave velocity inversion in monopole acoustic logging. Given the close interrelationship among P-wave velocity, density, and S-wave velocity [6], we opt to invert these three parameters simultaneously to enhance the stability and accuracy of the inversion algorithm. First, we analyze the feasibility of S-wave velocity inversion in soft formations. Next, we employ an analytical algorithm to synthesize full-waveform curves and construct a dataset. Ultimately, we develop a 1D-CNN to achieve the inversion of formation P-wave velocity, S-wave velocity, and density.

Feasibility Analysis of Inversion for S-wave Velocity

Fig. 1 illustrates a monopole acoustic logging model. In this model, the cylinder represents the well hole. The transmitter located at the origin serves as a point-expanding acoustic source. The dashed lines in the figure depict the propagation paths of the head waves that first arrive at the receivers. The acoustic pressure expression at the borehole axis is given as

DOI 10.5162/Ultrasonic2025/E2-a2

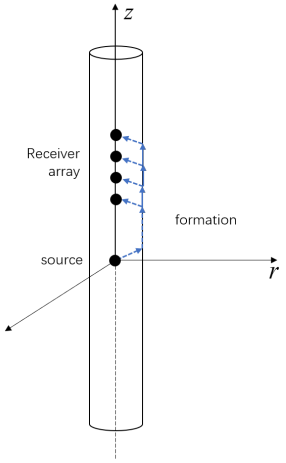

Fig. 1: Monopole acoustic logging model

follows [7],

$$p(z,t) = \frac{1}{2\pi^2}\int_{-\infty}^{\infty}\left[\frac{e^{ik_z z}}{z} + \frac{1}{\pi}\int_{-\infty}^{\infty} A(k_z,\omega)\, e^{ik_z z} dk_z\right] \times X(\omega)\, e^{-i\omega t} d\omega. \tag{1}$$

Among them, p represents the acoustic pressure at the well axis, $X(\omega)$ represents the frequency spectrum of the time function of the acoustic source, and $A(k_z,\omega)$ is the reflection coefficient of the wellbore wall. The expressions for S-wave velocity and P - wave velocity are respectively as follows,

$$v_s = \sqrt{G/\rho}, \tag{2}$$

$$v_p = \sqrt{(\lambda + 2G)/\rho}. \tag{3}$$

The low-frequency approximation formula for the phase velocity of Stoneley waves in the elastic formation surrounding the wellbore is presented as follows [8],

$$v_t{}^2 = \frac{v_f{}^2}{1 + \frac{\lambda+2G}{G}}. \tag{4}$$

Here, v_s represents the S-wave velocity of the formation outside the borehole, v_p is the P-wave velocity of the formation outside the borehole, v_f denotes the velocity of the fluid inside the borehole, v_t stands for the Stoneley wave velocity, G is the shear modulus of the formation, λ is the Lamé parameter of the formation, and ρ is the density of the formation. The shear modulus appears not only in the expression for S-wave velocity but also in those for P-wave and Stoneley-wave velocities. From the expression for S-wave velocity, it can be seen that when the density is fixed, the S-wave velocity varies with the shear modulus. Consequently, it can be inferred that the waveforms of both P-waves and Stoneley waves contain information related to the formation shear modulus.

Tab. 1: Wellbore fluid and formation parameters

	ρ (kg/m^3)	v_p (m/s)	v_s (m/s)
Wellbore fluid	1000	1500	–
Formation 1	2000	2300	900
Formation 2	2000	2300	1100

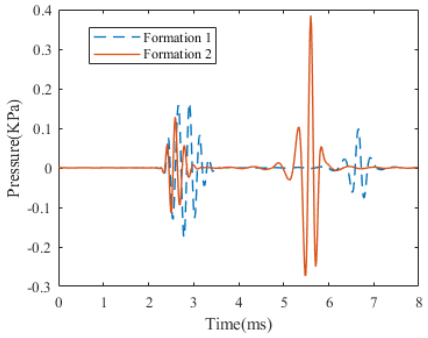

Fig. 2: Comparison of full-wave curves in soft formation

Then, the full-waveform curves of the acoustic pressure received at the well axis under two different soft formation conditions were calculated using the real-axis integration method [9]. The only difference between formation 1 and formation 2 is the S-wave velocity. The parameters of the fluid within the wellbore and the formations surrounding the wellbore are presented in Tab. 1. The radius of the wellbore is 0.1 m. The acoustic source is a cosine envelope pulse with a center frequency of 6 kHz and a half bandwidth of 4 kHz. The acoustic pressure amplitude at a distance of 0.01 m from the acoustic source was set to 100 kPa. In Fig. 2, the solid line represents the full acoustic pressure wave waveform curve received when the formation surrounding the borehole is Formation 2. As shown in Fig. 2, the first arrival is the critically refracted P-wave, followed by the Stoneley wave. In contrast, the dashed line depicts the acoustic pressure waveform corresponding to Formation 1. It can be seen that there is no S-wave waveform in Fig. 2. However, when the S-wave velocity is reduced from 1100 m/s to 900 m/s while keeping the other parameters of the formation unchanged, the amplitude of the P-wave increases and its duration becomes longer, while the amplitude of the Stoneley wave decreases and its arrival time becomes earlier. Clearly, both the P-wave and the Stoneley wave are related to the S-wave velocity. Some scholars have attempted to invert the S-wave velocity of the formation from the characteristics of the P-wave and the Stoneley wave. For example, Zhou [10] used the amplitude of the P-wave to solve for the S-wave velocity in the formation.

DOI 10.5162/Ultrasonic2025/E2-a2

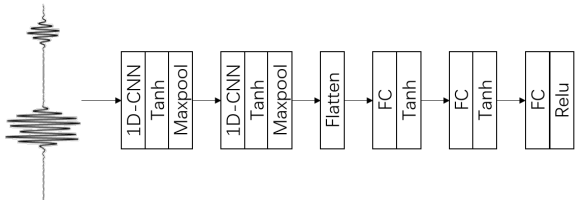

Fig. 3: 1D-CNN model

Wu [3] inverted the S-wave velocity of the formation using the low-frequency approximation formula of the Stoneley wave velocity obtained under different formation medium models and logging acoustic systems.

Although variations in S-wave velocity can induce changes in the full - waveform curve, the relationship between them is difficult to represent using a single characteristic of the wave. Therefore, we establish the relationship between the full - waveform curve and S-wave velocity with the aid of a one - dimensional Convolutional Neural Network (1D-CNN). Even when the receiver in a soft formation fails to detect a separate S wave, it is expected to invert the S-wave velocity from the waveforms of P-waves and Stoneley waves by 1D-CNN.

1D-CNN for Formation Parameters Inversion

This paper, based on the monopole acoustic logging model shown in Fig. 1, employs the real-axis integration method to compute multiple full-waveform curves using P-wave velocity, S-wave velocity, density, and other borehole parameters. In the dataset, we calculated full-waveform curves not only in soft formations but also in hard formations, with the expectation that the 1D-CNN could simultaneously invert the P-wave and S-wave velocities as well as the density of both soft and hard formations. These curves are then consolidated into a dataset comprising a total of 24,754 entries. During neural network training, 80% of the data from the dataset is randomly selected as the training set, 10% as the validation set, and the remaining 10% as the test set.

The one-dimensional convolutional neural network (1D-CNN) constructed in this paper is illustrated in Fig. 3. In the 1D-CNN, the input size is set to 1024*1, where 1024 represents the length of the input full-waveform curve. The output size is 3*1, corresponding to a set of values for P-wave velocity, S-wave velocity, and density. In Fig. 3, the first convolutional layer employs 64 convolutional kernels of size 16*1 to extract features from the full-waveform curve, yielding feature maps without additional padding. The second convolutional layer, also with 64 convolutional kernels of size 16*1, is connected to the pooled output of the first convolutional layer, again without additional padding. The first fully connected layer consists of 32 neurons and takes the flattened features from the last convolutional layer as input. The second fully connected layer has 16 neurons. The third fully connected layer, with 3 neurons, outputs the P-wave velocity, S-wave velocity, and density in the form of a 3*1 vector. The stride for convolution in all convolutional layers is set to 1. Max-pooling is employed in all pooling layers, with a kernel size of 8*1 and a stride of 4. The activation functions in the first to fourth activation function layers are the tanh function, $\tanh(x) = \frac{e^x - e^{-x}}{e^x + e^{-x}}$. The activation function in the fifth activation function layer is the ReLU function, with the expression $f(x) = \max(0, x)$. The loss function is as follows:

$$L = (L_s + L_p + L_\rho)/3 \tag{5}$$

where

$$\begin{aligned} L_s &= \frac{1}{N}\sum_{i=1}^{N}\left(S_i - \hat{S}_i\right)^2 \\ L_p &= \frac{1}{N}\sum_{i=1}^{N}\left(P_i - \hat{P}_i\right)^2 \\ L_\rho &= \frac{1}{N}\sum_{i=1}^{N}\left(\rho_i - \hat{\rho}_i\right)^2 \end{aligned} \tag{6}$$

Here, L represents the loss function. L_s, L_p, and L_ρ denote the mean squared errors of S-wave velocity, P-wave velocity, and density, respectively. S_i and $\hat{S}_i$ represent the actual and predicted values of S-wave velocity, respectively. P_i and $\hat{P}_i$ represent the actual and predicted values of P-wave velocity, respectively. ρ_i and $\hat{\rho}_i$ represent the actual and predicted values of density, respectively. During network training, the number of training epochs is set to 150, and the batch size is 128. The Adam optimizer [11] is selected to optimize the network weights in order to minimize the loss function. The initial learning rate is 0.001. If the loss function on the validation set does not decrease for 5 consecutive training epochs, the learning rate is halved.

Results

After training, the 1D-CNN has learned the relationships between the full-waveform curves and the P-wave velocity, S-wave velocity, and density. When performing formation velocity inversion, 1D-CNN do not require pre - processing of the full - waveform curve. Running on a processor (i7-8700) and a graphics card (GeForce GTX 1050 Ti), the 1D-CNN takes only 3 milliseconds to predict a set of P-wave velocity, S-wave velocity, and density values. We use the relative error for evaluation, and its formula is $\delta = \left|y_i - \widehat{y_i}\right| / y_i \times 100\%$, y_i represents the actual value, and $\widehat{y_i}$ represents the predicted value. On the

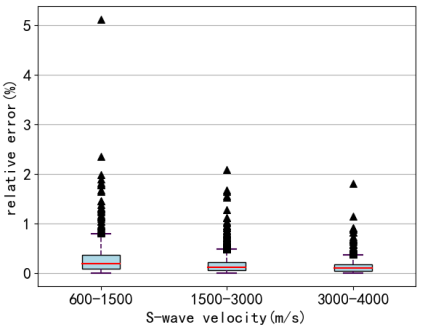

Fig. 4: Box plot of relative error in S-wave velocity

test set, the average relative errors of the S-wave velocity, P-wave velocity, and density predicted by the 1D-CNN are 0.187%, 0.122%, and 0.265%, respectively. The box plot of the relative errors in the inverted S-wave velocities is presented in Fig. 4. The triangles in the graph represent outliers within the relative error data. In soft formations, only three outliers exceeded 2%. In the box plot, the red line represents the median of the relative error. Softer formations exhibit larger relative errors and more outliers compared to harder formations. Nevertheless, the average relative error in the inverted S-wave velocity for soft formations is still very small (0.335%), with 99.4% of the S-wave velocities having relative errors within 2%, indicating that the inverted values are very close to the actual values. The 1D-CNN demonstrates high accuracy in inverting S-wave velocities, with errors fluctuating within a narrow range.

Conclusion

This paper employs a 1D-CNN to simultaneously invert the formation's P-wave velocity, S-wave velocity, and density from the full-waveform curves of monopole acoustic logging. The trained 1D-CNN achieves average relative errors of 0.187%, 0.122%, and 0.265% for S-wave velocity, P-wave velocity, and density, respectively, on the test set. It demonstrates high accuracy with errors fluctuating within a narrow range. The average relative error in the inverted S-wave velocity for soft formations is very small (0.335%), with 99.4% of the S-wave velocities having relative errors within 2%. When the formation is soft, even if the receiver on the borehole axis cannot receive the S-wave, the 1D-CNN can still effectively invert the formation's S-wave velocity from the acoustic pressure full-waveform curves.

Acknowledgments

We acknowledge the financial support by the National Science Foundation of China (NSFC-12472087 and NSFC-12272107).

References

[1] Z. Ma and J. Xie. "Study on the Relationship Between Longitudinal Wave Velocity, Shear Wave Velocity, and Density of Rocks". In: *Progress in Geophysics* 20.4 (2005), pp. 905–910.

[2] K. Wang, Z. Cui, R. Song, et al. "Theoretical Proof That the First Arrival of Shear Wave in Acoustic Logging of Soft Formations Is an Evanescent Wave". In: *Proceedings of the Chinese Geophysical Society*. 2009, p. 126.

[3] X. Wu, S. Yu, and K. Wang. "Method and Application Research on Inversion of Formation Shear Wave Velocity Using Stoneley Wave Velocity". In: *Chinese Journal of Geophysics* 38.S1 (1995), pp. 216–223.

[4] C. H. Cheng. "Full waveform inversion of P waves for Vs and Qp". In: *Journal of Geophysical Research* 94.B11 (1989), pp. 15619–15625.

[5] I. Goodfellow, Y. Bengio, and A. Courville. *Deep Learning*. MIT Press, 2016. ISBN: 978-0262035613.

[6] Q. Li. "The Relationship Between Longitudinal Wave Velocity and Shear Wave Velocity of Rocks". In: *Geophysical Prospecting for Petroleum* 27.1 (1992), pp. 1–12+154.

[7] L. Tsang. "Numerical Evaluation of Transient Acoustic Waveform Due to a Point Source in a Fluid-Filled Borehole". In: *Geophysics* 44 (1979), pp. 1706–1727. DOI: 10.1190/1.1441020.

[8] M. A. Biot. "Propagation of Elastic Waves in a Cylindrical Bore Containing a Fluid". In: *Journal of Applied Physics* 23.9 (1952), pp. 997–1005. DOI: 10.1063/1.1702365.

[9] J. E. White and R. E. Zechman. "Computed Response of an Acoustic Logging Tool". In: *Geophysics* 33.2 (1968), pp. 302–310. DOI: 10.1190/1.1439927.

[10] S. Zhou, K. Wang, J. Ma, et al. "Application Research of Generalized Linear Inversion Method for Obtaining V_S and Q_P Values Using Borehole First Arrival Waves". In: *Chinese Journal of Geophysics* 38 (1995). suppl., pp. 242–252.

[11] D. P. Kingma and J. Ba. "Adam: A Method for Stochastic Optimization". In: *International Conference on Learning Representations*. 2014.